Inorganica Chimica Acta, 202 (1992) 37–41

Synthesis, characterization and molecular structure of the 1-methylimidazolium carbonyl-1-methylimidazoletetrachlororuthenate(III)

Alzir Azevedo Batista*, Lis Regina V. Olmo
Departamento de Química, Universidade Federal de São Carlos, Rodovia Washington Luiz Km 235, São Carlos, SP (Brazil)

Glaucius Oliva, E. E. Castellano and Otaciro R. Nascimento
Departamento de Física e Ciência dos Materiais, Instituto de Física e Química de São Carlos, Av. Carlos Botelho 1465, São Carlos, SP (Brazil)

(Received April 10, 1992; revised June 24, 1992)

Abstract

The complex M-ImH[RuCl$_4$(CO)(M-Im)], where M-Im = 1-methylimidazole = $C_4N_2H_6$, was synthesized and found to crystallize in the space group $P2_1/n$, with $a = 7.631(2)$, $b = 10.832(3)$, $c = 19.389(4)$ Å, $\beta = 91.52°$ and $Z = 4$. The structure was solved from 1600 independent reflections with $I > 3\sigma(I)$ by Patterson and difference Fourier techniques and refined to $R = 0.038$. The Ru(III) ion is octahedrally coordinated to four co-planar chlorine atoms, the carbon atom of a CO group and a nitrogen of an M-Im ring. Another protonated M-Im group, which forms the counter-cation completes the crystal structure. The UV-Vis absorption spectrum shows two bands (316 and 442 nm) associated with ligand-to-metal charge transfer transitions and a third band at lower energy (530 nm) was assigned to a d–d transition. Room and liquid nitrogen temperatures EPR data confirmed the presence of the paramagnetically active Ru(III) and is consistent with the slightly distorted local C_{4v} symmetry of the complex. The position of the stretching CO band is discussed in terms of metal–CO backbonding. The EPR data, measured at two frequencies (X and Q bands) show a rhombic distortion in the structure of the complex.

Introduction

Low-valent ruthenium complexes that contain tertiary phosphine ligands have been used in the area of homogeneous catalysis [1, 2]. Some of these complexes contain carbonyl ligands and their catalytic activities for hydrogenation of unsaturated organic substrates have been reported [3, 4]. In the course of the synthesis of the carbonyl-*N*-heterocyclic complex RuCl$_2$(CO)$_2$(M-Im)$_2$, an effective catalyst in hydrogenation reactions [5], a new Ru(III) complex, M-ImH[RuCl$_4$(CO)(M-Im)] was obtained. Recently, M-ImH(*trans*-RuCl$_4$Im$_2$) was reported in the literature and its tumor-inhibiting properties were described [6]. Because of the similarity of the structure of these compounds and the simple method of synthesis of this new complex, an extensive characterization was undertaken. Furthermore the structure determination and more complete spectroscopic studies could contribute to a better understanding of the chemistry of this kind of Ru(III) compound. This complex of carbon monoxide is very stable, even in solution, also making it potentially useful for catalytic oxidation reactions.

Experimental

Preparation

Commercial (Degussa) hydrated ruthenium trichloride (1.00 g 3.80 mmol), was dissolved in methanol (10 ml) and a stream of carbon monoxide was passed through it, at room temperature. The initial deep red–brown solution turned deep, clear red after 48 h. To this solution, M-Im (0.63 g, 7.60 mmol) was added and stirring was continued overnight under argon. The red crystals which formed were collected by filtration, washed with methanol and dried under vacuum. Recrystallization from ethanol–diethyl ether afforded the product as very bright red crystals.

Elemental analysis

Standard microanalyses were performed on crystalline samples. Calc.: C, 24.8; H, 3.0; N, 12.8. Found: C, 24.8; H, 3.1; N, 13.0%.

---

*Author to whom correspondence should be addressed.

0020-1693/92/$5.00

X-ray diffraction data

A complete data set was collected on an Enraf-Nonius CAD-4 four cicle diffractometer, from a flat prismatic crystal. Experimental details are given in Table 1. Cell dimensions and the orientation matrices were calculated by least-squares from 25 centered reflections. Diffraction intensities were measured by the ω–2θ scan technique using a variable scan speed of 6.7–20.0° $\min^{-1}$ determined by a pre-scan at 20.0° $\min^{-1}$. The intensity of one standard reflection was essentially constant over the duration of the experiments. Data were corrected for Lorentz, polarization and absorption effects, following the procedure of Walker and Stuart [7]. From the 2477 unique reflections measured, the 1600 having $I > 3\sigma(I)$ were used for the structure determination and refinement. These were performed with the SHELX76 [8] system of programs. Bonded H-atom scattering factors [9] and complex scattering factors [10, 11] were employed for the remaining atoms. Figure 1 was drawn with the ORTEP [12] program.

Crystal structure determination and refinement

The structure was solved by standard Patterson and difference Fourier techniques and refined by full-matrix least-squares methods with anisotropic thermal parameters for the non-hydrogen atoms. All hydrogen atoms were located from difference Fourier maps and included as fixed contributors, with one refined common isotropic temperature factor for the methyl hydrogens 5.0(8) Å^2 and another for the remaining ones 10(1) Å^2. See also 'Supplementary material'.

TABLE 1. Crystal data, data collection details and structure refinement results for M-ImH[$RuCl_4$(CO)(M-Im)]

Formula	$N_2C_4H_7[RuCl_4(CO)(N_2C_4H_6)]$
Molecular weight	435.1
Space group	$P2_1/n$
Lattice parameters	
a (Å)	7.631(2)
b (Å)	10.832(3)
c (Å)	19.389(4)
β (°)	91.52(2)
V (A^3)	1602(1)
Z	4
D_{calc} (g cm^{-3})	1.804
Sample dimensions (mm)	$0.05 \times 0.15 \times 0.23$
Radiation, λ (Å)	Mo Kα, 0.71073
T (°C)	25
Linear absorption coefficient, μ (mm^{-1})	1.63
Transmission factors: max., min	1.118, 0.886
Scan technique	ω–2θ
Scan speed range (° min^{-1})	6.7–20
θ range for data collection (°)	0–25
$F(000)$	856
No. independent reflections	2477
No. reflections above $3\sigma(I)$	1600
No. refined parameters	175
Minimized function	$\Sigma w(\lvert F_o\rvert - \lvert F_c\rvert)^2$
Weighting scheme	$w = [\sigma^2(\lvert F_o\rvert) + 0.001\lvert F_o\rvert^2]^{-1}$
$R = \Sigma\lVert F_o\rvert - \lvert F_c\rVert/\Sigma\lvert F_o\rvert$	0.038
$R_w = [\Sigma w(\lvert F_o\rvert - \lvert F_c\rvert)^2/\Sigma w\lvert F_o\rvert^2]^{1/2}$	0.040
$S = [\Sigma w(\lvert F_o\rvert - \lvert F_c\rvert)^2/(M-N)]^{1/2}$	1.03
h_{min}, h_{max}; k_{min}, k_{max}; l_{min}, l_{max}	−9, 9; 0, 12; 0, 22
Max, min. residual ρ (e Å^{-3})	0.53, −0.51

Spectroscopic measurements

IR spectra

Pellets were prepared from crystalline powder samples diluted in CsI. Measurements were performed on a Bomem-Michelson 102 spectrometer in the region 4000–190 cm^{-1}.

UV–Vis spectra

The electronic spectrum was measured in CH_2Cl_2 solution (8×10^{-5} mol/l) on a Varian DMS-100 spectrophotometer.

EPR measurements

EPR spectra were obtained from a polycrystalline powder sample, using a quartz tube, on a Varian E-109 spectrometer equipped with X and Q band bridges at room and at liquid nitrogen temperatures. For measuring conditions see Fig. 4.

Electrochemistry

The cyclic voltammogram was recorded at 25.0±0.1 °C in freshly distilled dichloromethane with 0.1 mol/l of tetrabutylammonium perchlorate (TBAP) using an EG & PARC electrochemical system consisting of a model RE 0073 recorder, a model 173 potentiostat and a model 175 universal programmer. A three electrode system consisting of glassy carbon working and a platinum auxiliary electrode was used. The reference electrode was Ag/AgI (TBAP 0.2 mol/l in CH_2Cl_2). The working solution was separated from the reference electrode with a Luggin-Haber containing salt bridge, filled with the solvent and supporting electrolyte. Temperature was stabilized with the electrochemical cell immersed in a constant temperature bath. As recommended by IUPAC [13], the ferrocinium (Fc^+)/ferrocene (Fc) couple was employed as the internal reference and all potentials reported herein are given in relation to the oxidation potential of the reference electrode (0.55 V). TBAP (Fluka purum) was recrystallized from ethanol/water and dried under vacuum at 100 °C overnight. Dichloromethane was distilled over P_2O_5 and stored over Linde 4 Å molecular sieves. All working solutions were degassed with prepurified argon before measurements and were kept under an argon blanket during the experiments.

Magnetic susceptibility

Solution magnetic susceptibility was measured by the Evans NMR method [14], with a 60 MHz Varian instrument, using CH_2Cl_2 solution at room temperature.

Electrical conductivity

Solution electrical conductivity was measured in nitromethane at 25 °C under anaerobic conditions using a Micronal conductivity bridge.

Results and discussion

Fractional and equivalent isotropic temperature factors for all non-H atoms are given in Table 2 and interatomic bond distances and angles are in Table 3. Figure 1 is a drawing of the complex showing the labelling of non-H atoms and their thermal vibration ellipsoids. See also 'Supplementary material'. The Ru(III) ion is octahedrally coordinated to four coplanar chlorine atoms, a carbon atom of a CO group and a nitrogen of an M-Im ring. Another M-Im group, protonated, presents an electrostatic interaction completing the crystal structure of the complex.

The Ru–Cl and Ru–N bond lengths in the M-ImH[RuCl$_4$(CO)(M-Im)] complex are comparable to those found for the ImH(*trans*-RuCl$_4$(Im)$_2$) complex (*c*. 2.35 and 2.079 Å, respectively) or for 4-M-Im[*trans*-RuCl$_4$(4-M-Im)$_2$] (*c*. 2.36 and 2.08 Å) [6]. The bond length for the Ru–N present in the M-ImH[RuCl$_4$(CO)(M-Im)] complex, 2.12 Å, reflects the backbonding of the Ru–CO interaction, making the Ru–N length longer compared with those found for the related complexes above.

TABLE 2. Fractional atomic coordinates and isotropic temperature parameters (Å^2) of M-ImH[RuCl$_4$(CO)(M-Im)]

Atom	*x/a*	*y/b*	*z/c*	B_{iso}
Ru	−0.2133(1)	0.2124(1)	0.1100(0)	2.72(2)
Cl(1)	0.0549(2)	0.2159(2)	0.0541(1)	4.18(7)
Cl(2)	−0.4862(3)	0.2019(2)	0.1621(1)	4.24(7)
Cl(3)	−0.2793(2)	0.0185(2)	0.0595(1)	3.42(6)
Cl(4)	−0.1611(3)	0.4081(2)	0.1580(1)	4.64(8)
C(1)	−0.106(1)	0.1378(8)	0.1871(5)	4.4(3)
O(1)	−0.041(1)	0.0925(7)	0.2337(4)	7.4(3)
N(11)	−0.3321(7)	0.2994(5)	0.0223(3)	2.8(2)
N(12)	−0.3619(8)	0.4184(6)	−0.0683(3)	3.3(2)
C(11)	−0.2549(9)	0.3832(7)	−0.0170(4)	3.4(3)
C(12)	−0.4969(9)	0.2830(8)	−0.0059(4)	3.8(3)
C(13)	−0.5169(9)	0.3557(9)	−0.0616(5)	4.2(3)
C(14)	−0.321(1)	0.5069(8)	−0.1226(5)	5.4(4)
N(21)	−0.3210(9)	0.0620(7)	−0.1200(4)	4.3(3)
N(22)	−0.1083(8)	0.1729(6)	−0.1526(4)	3.9(2)
C(21)	−0.165(1)	0.1033(8)	−0.1014(4)	3.8(3)
C(22)	−0.367(1)	0.1036(9)	−0.1833(5)	4.5(3)
C(23)	−0.234(1)	0.1716(8)	−0.2046(4)	4.3(3)
C(24)	0.064(1)	0.237(1)	−0.1547(6)	6.8(5)

TABLE 3. Interatomic bond distances (Å) and angles (°) of M-ImH[RuCl$_4$(CO)(M-Im)]

Bond distances		Bond angles	
Ru–Cl(1)	2.341(2)	Cl(1)–Ru–Cl(2)	177.28(8)
Ru–Cl(2)	2.341(2)	Cl(1)–Ru–Cl(3)	90.11(7)
Ru–Cl(3)	2.366(2)	Cl(1)–Ru–Cl(4)	91.59(8)
Ru–Cl(4)	2.345(2)	Cl(1)–Ru–C(3)	90.4(3)
Ru–C(3)	1.869(9)	Cl(1)–Ru–N(11)	89.0(2)
Ru–N(11)	2.126(6)	Cl(2)–Ru–Cl(3)	87.33(7)
C(3)–O	1.13(1)	Cl(2)–Ru–Cl(4)	90.94(8)
N(11)–C(11)	1.33(1)	Cl(2)–Ru–C(3)	90.6(3)
N(11)–C(12)	1.370(9)	Cl(2)–Ru–N(11)	90.1(2)
N(12)–C(11)	1.33(1)	Cl(3)–Ru–Cl(4)	177.21(8)
N(12)–C(13)	1.37(1)	Cl(3)–Ru–C(3)	91.8(3)
N(12)–C(14)	1.46(1)	Cl(3)–Ru–N(11)	88.9(2)
C(12)–C(13)	1.34(1)	Cl(4)–Ru–C(3)	90.4(3)
N(21)–C(21)	1.31(1)	Cl(4)–Ru–N(11)	88.9(2)
N(21)–C(22)	1.35(1)	C(3)–Ru–N(11)	179.1(3)
N(22)–C(21)	1.33(1)	Ru–C(3)–O	179.9(8)
N(22)–C(23)	1.37(1)	Ru–N(11)–C(11)	125.0(5)
N(22)–C(24)	1.49(1)	Ru–N(11)–C(12)	129.0(5)
C(22)–C(23)	1.33(1)	C(11)–N(11)–C(12)	106.0(6)
		C(11)–N(12)–C(13)	107.6(6)
		C(11)–N(12)–C(14)	126.1(7)
		C(13)–N(12)–C(14)	126.3(7)
		N(11)–C(11)–N(12)	110.6(6)
		N(11)–C(12)–C(13)	109.2(7)
		N(12)–C(13)–C(12)	106.6(7)
		C(21)–N(21)–C(22)	110.4(7)
		C(21)–N(22)–C(23)	107.9(7)
		C(21)–N(22)–C(24)	126.2(7)
		C(23)–N(22)–C(24)	125.8(7)
		N(21)–C(21)–N(22)	107.4(7)
		N(21)–C(22)–C(23)	106.6(8)
		N(22)–C(23)–C(22)	107.6(8)

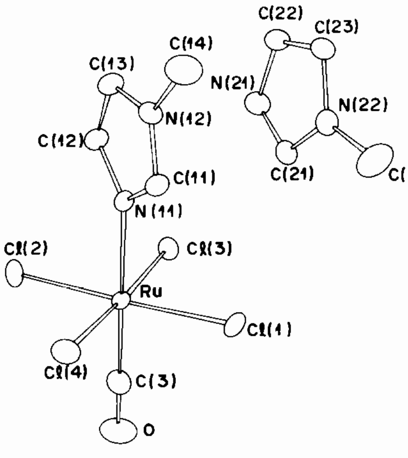

Fig. 1. Molecular structure and crystallographic numbering scheme for M-ImH[RuCl$_4$(CO)(M-Im)].

The strong absorption band in the IR spectrum at 2037 cm^{-1} corresponding to the ν(CO) stretch, is shifted with respect to the CO absorption band, 2143 cm^{-1}

[15], indicating a small amount of metal–CO back-bonding. This is also consistent with the slightly larger C–O bond distance in the complex (1.13 Å), when compared to the free molecule, 1.10 Å [16]. The Ru–Cl stretching frequency was also observed, at 325 cm^{-1}. The bands present at 760(s) and 1075(s) cm^{-1} and at 739(s) and 1103(s) cm^{-1} are related to protonated and coordinated ligands, respectively. These respective bands for the Im-H[$RuCl_4(Im)_2$] complex are at 622 and 1050 cm^{-1} and at 612 and 1069 cm^{-1}, for the protonated and coordinated imidazole, respectively.

The electronic absorption spectrum (Fig. 2) shows three bands. The two higher energy transitions at 316 nm ($\epsilon = 1182\ M^{-1}\ cm^{-1}$) and 442 nm ($\epsilon = 3220\ M^{-1}\ cm^{-1}$) can be assigned as ligand-to-metal charge transfer (LMCT) transitions. On the basis of the observed C_{4v} symmetry of the complex, the band at lower energy 530 nm ($\epsilon = 390\ M^{-1}\ cm^{-1}$) can be tentatively assigned to the d–d transition $^1A_1 \rightarrow {}^1B_2$, according to the energy-levels proposed by Sacconi and co-workers [17].

Cyclic voltammetric measurements (Fig. 3) on the complex using a glassy carbon working electrode, resulted in two well-behaved reversible waves representing Ru(III)/Ru(II) and Ru(II)/Ru(I) redox couples, where the $E_{1/2}$ values are 0.85 and 0.47 V, respectively, versus Fc^+/Fc. This assumption of a two-step one-electron process is consistent with other Ru(III)/Ru(II), Ru(II)/Ru(I) systems reported in the literature [18].

The solution μ_{eff} value for the complex yielded a spin-only value of 1.72 μ_B being consistent with one unpaired electron per atom of ruthenium. The molar conductivity data obtained for the complex in nitromethane 64 $\Omega^{-1}\ cm^2\ mol^{-1}$ is consistent with a 1:1 electrolyte [19].

The EPR spectra measured at two frequencies (X and Q bands) show a rhombic distortion in the structure. This rhombic distortion increases if the temperature is lowered to 77 K (Fig. 4). Using a simulation program for powder spectra the EPR parameters were obtained and a strong and anisotropic variation of linewidths are observed especially for the g_1 line ($g_1 < g_2 < g_3$). The changes in the EPR parameters with temperature (Table 4) indicate the sensitivity of the d–d orbital mixture with the coupling of the vibrational modes via a

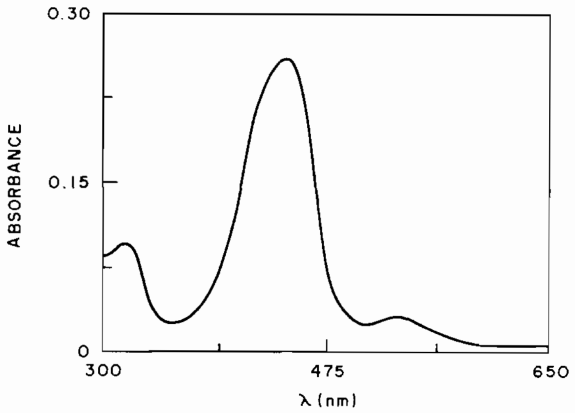

Fig. 2. Absorption spectrum of M-ImH[$RuCl_4(CO)(M\text{-}Im)$] complex in the near UV–Vis region in CH_2Cl_2, 8.0×10^{-5} mol/l.

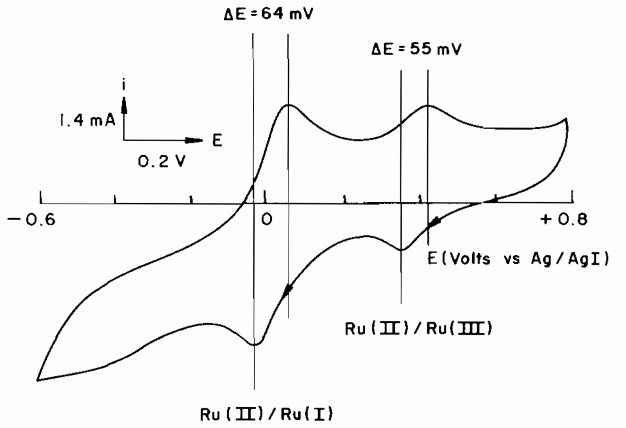

Fig. 3. Cyclic voltammogram of 3.6×10^{-4} mol/l M-ImH[$RuCl_4(CO)(M\text{-}Im)$] in Ch_2Cl_2 (0.2 mol/l TBAP) measured at a glassy carbon electrode. Scan rate 75 mV s^{-1}. $Fc^+/Fc = 0.55$ V vs. Ag/AgI electrode.

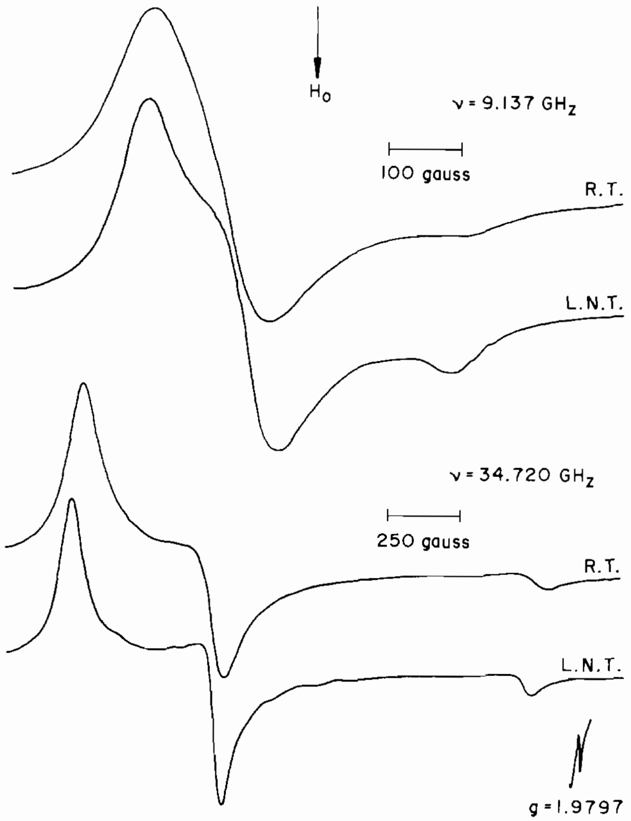

Fig. 4. EPR spectra of M-ImH[$RuCl_4(CO)(M\text{-}Im)$] (X and Q bands) at room and liquid nitrogen temperatures. Modulation amplitude: 5 gauss. Microwave power: 20 mW.

TABLE 4. EPR parameters of the M-ImH[$RuCl_4$(CO)(M-Im)] complex

	g_1	g_2	g_3	Temperature (K)
X band	2.0027	2.2103	2.2928	300
	2.0060	2.2040	2.3045	77
Q band	2.0017	2.2068	2.2940	300
	2.0065	2.1980	2.2955	77

spin–orbit interaction. The strong change in the linewidth of g_1 is associated with the CO and methylimidazole groups.

Supplementary material

A list comparing observed and calculated structure factors, the parameters of the non-H atoms' ellipsoids, and the H atoms' atomic coordinates and temperature factors are available from the authors on request.

References

1 B. R. James, *Homogeneous Hydrogenation,* Wiley, New York, 1973, p. 72.
2 E. Seddon, *The Chemistry of Ruthenium,* Elsevier, New York, 1984, pp. 1373.
3 D. R. Fahey, *J. Org. Chem., 38* (1973) 3343.
4 R. Vac, J. H. Nelson, E. B. Milosavljevic' and L. Solujic', *Inorg. Chem., 28* (1989) 3831.
5 A. A. Batista, L. R. V. Olmo, G. Oliva, E. E. Castellano and O. R. Nascimento, *7th Int. Symp. Homogeneous Catalysis, Lyon, France, 1990,* p. 142.
6 B. K. Keppler, W. Ruph, U. M. Juhl, H. Endres, R. Niebl and W. Balzer, *Inorg. Chem., 26* (1987) 4366.
7 N. Walker, D. Stuart, *Acta Crystallogr., Sect. A., 39* (1983) 158.
8 G. M. Sheldrick, *SHELX,* a program for crystal structure determination, University of Cambridge, Cambridge, UK, 1976.
9 R. F. Stewart, E. R. Davison and W. T. Simpson, *J. Chem. Phys., 42* (1965) 3175.
10 D. T. Cromer and D. Liberman, *J. Chem. Phys., 53* (1970) 1891.
11 D. T. Cromer and J. B. Mann, *Acta Crystallogr., Sect. A, 24 (1968) 321.*
12 C. K. Johnson, ORTEP, *Rep. ORNL-3794,* Oak Ridge National Laboratory, TN, USA, 1965.
13 G. Gritzner and J. Kuta, *Pure Appl. Chem., 54* (1982) 1528.
14 D. F. Evans, *J. Chem. Soc.,* (1959) 2003.
15 Ch. Elschenbroich, A. Salzer, *Organometallics — A Concise Introduction,* VCH, Weinheim, Germany, 1989, p. 229.
16 A. Yamamoto, *Organotransition Metal Chemistry — Fundamental Concepts and Applications, Wiley,* New York, 1978, p. 642.
17 M. Bacci, S. Midollini, P. Stoppioni and L. Sacconi, *Inorg. Chem., 12* (1973) 1801.
18 E. B. Milosavljevic', L. J. Solujic', D. W. Krassowski and J. H. Nelson, *J. Organomet. Chem., 352* (1988) 177.
19 W. J. Geary, *Coord. Chem. Rev., 7* (1971) 81.